Inversion of Optical Reflectance in the Fullerenes

F. Marsiglio
Department of Physics, University of Alberta, Edmonton, AB T6G 2J1

Since the discovery of superconductivity in the alkali-doped fullerenes [1], the electron-phonon interaction has been the primary suspect for superconductivity in this class of compounds. In this paper we first provide a pedagogical review of how the question of mechanism has traditionally been settled, and then some well-known properties of the optical reflectance (and the derived conductance) are summarized. Finally we demonstrate how a recently derived inversion procedure can use the optical properties of a metal to infer the magnitude of the electron-phonon interaction. We conclude that in the case of the alkali-doped fullerenes, the electron-phonon interaction is sufficiently strong to explain the transition temperatues found in these the materials.

Introduction

The fcc solid composed of C_{60} molecules at the lattice sites is an insulator, and almost certainly a band insulator [2]. As is the case with graphite, this material can be doped with alkali metal atoms. One can try for various 'stoichiometric' results, such as A_nC_{60}, where A is an alkali metal atom, and n is an integer ranging from 1 through 6. Various interesting phases result, as a function of n (and to a lesser extent A). In some cases, the compound apparently doesn't form, with indications of phase separation at low temperature (see Ref. [3], for example). The point of interest for us is $n = 3$, for it is at this doping level (and apparently only this doping level) that superconductivity occurs. Unlike the focus of much of the work in high temperature superconducting cuprate materials (which also have an insulating parent state), it appears to be a much more difficult problem here to relate the various phases that occur as a function of n. Here the situation is intrinsically different, in that only stoichiometric compounds form (although suggestions that this may also be the case in the cuprates have appeared from time to time). Thus, for this work we relinquish the 'big picture', and focus only on A_3C_{60}, and in particular, A = K, which is a superconductor with a transition temperature, $T_c = 20$ K.

There are many indications [3,4] that the K_3C_{60} compounds are (a) well-behaved Fermi Liquids, and (b) conventional electron-phonon superconductors. Property (a) does not imply property (b), although property (b) presupposes that (a) is true. The main indication that Fermi Liquid theory (FLT) might be the appropriate starting point is the temperature dependence of the resistivity, which exhibits the standard FLT behaviour, $\rho(T) = a+bT^2$ [5]. Various measurements below the critical temperature indicate that the superconducting state is a conventional s-wave one. Gap measurements, using both tunneling and infrared spectroscopy [6–8] indicate an s-wave gap, though there is some controversy over the size of the gap. The existence of an s-wave gap is also supported by penetration depth measurements [10]. Furthermore, a coherence peak in the spin relaxation rate, $1/T_1$, has been measured using muons [9], a result which lends strong support to an s-wave BCS picture. Finally, the isotope effect has been determined to be significant (see Ref. [11] for a summary), although again the size of the isotope exponent is controversial.

The Question of Mechanism

All of these measurements support the existence of an s-wave gap, but, with the exception of the isotope effect, have little to say about mechanism. Partly this is the "curse" of universality; BCS theory was so successful partly because it provided universal results (for various properties and temperature dependences). However, one consequence of this is that for a wide variety of mechanisms, if the coupling is weak, the prediction for many superconducting properties is the same. Hence, the theory is not very useful for discriminating mechanism. One can claim, for example, that in the case of Al (which is a very weak coupling superconductor), there is no definite proof for electron-phonon superconductivity [12]. For certain superconducting materials (known in the older literature as "bad actors") like Pb and Hg, deviations from universal behaviour were measured, so there was hope that these deviations could point towards a mechanism. This is exactly what happened in the case of Pb, particularly through tunneling experiments, as we will now describe.

In single particle tunneling experiments an (insulating) oxide layer is sandwiched between a superconducting material and a normal metal (other variants are possible, but we focus on this, the simplest). An external circuit allows electrons to tunnel across this barrier. If a single particle energy gap exists in the superconducting side, then no current will flow until the bias voltage exceeds this energy gap. In this way one can measure the energy gap in a superconductor (provided one exists). This is exactly what the original experiments by Giaever [13] measured (in an Al/Pb sandwich).

Actually, even this measurement indicated that something was wrong. The gap ratio, $2\Delta/k_BT_c$, was measured to be well over 4 (later more accurate measurements indicated a value closer to 4.5), whereas BCS theory predicts a universal result, 3.5. Strong coupling was suspected,

although strong coupling extensions of BCS theory only managed to raise this universal value to yet another universal maximum value, 4.0 [14]. By this time Eliashberg had extended the theory to include dynamical interactions with phonons [15]. As further refinements in both theory and experiment developed, it became clear that certain structure in the density of states (as measured by electron tunneling in Pb, one of the "bad actors") was due to the electron-phonon interaction [16,17]. Finally, McMillan and Rowell succeeded in using tunneling measurements and the Eliashberg equations to extract the underlying electron-phonon interaction in the form of the electron-phonon spectral function, $\alpha^2F(\Omega)$ [18,19]. We now describe qualitatively the essence of Eliashberg theory (for various reviews see Ref. [20–23]), and of the McMillan-Rowell inversion procedure.

Within BCS theory, the gap parameter $\Delta_{\rm BCS}$ serves both as an order parameter, and as the energy below which the density of states is zero (hence the name "gap" parameter). The only input required in the theory is a model attractive potential, multiplied by the electron density of states at the Fermi level: $N(\epsilon_F)V$. As already mentioned above, Eliashberg theory goes one step further; it recognizes that a source for the attraction is the electron-phonon interaction, and that retardation effects can be important since the mean ion velocity is significantly less than the Fermi velocity of the electrons. The result is that the source of attraction is encapsulated by an electron-phonon spectral function, $\alpha^2F(\Omega)$. Moreover, the order parameter in Eliashberg theory is frequency dependent. Finally, the direct electron-electron Coulomb repulsion is recognized as a source of depairing, and is generally included at a minimal level through a single dimensionless parameter, μ^*. The '$*$' is present to remind us that this is a pseudopotential, and ought to have a greatly reduced value if one uses cutoffs in the theory which apply to the phonon energy scale. To summarize, Eliashberg theory produces an equation analagous to the BCS one, except that the order parameter is a function of frequency ω, a functional of $\alpha^2F(\Omega)$, and a function of μ^*. It is also complex (not in the usual sense: this applies even if the phase has been set to zero). Once this gap function, $\Delta(\omega)$, is obtained, one can calculate a variety of properties, one of which is the single particle density of states, $N(\omega) = N(\epsilon_F){\rm Re}\left\{\frac{\omega}{\sqrt{\omega^2-\Delta^2(\omega)}}\right\}$. This expression bears a remarkable resemblance to the weak coupling result, for which the gap function would simply be replaced by the gap parameter, $\Delta_{\rm BCS}$. Note that the I-V characteristic is proportional to the single particle density of states: $dI(V)/dV \propto N(V)$, so that an I-V measurement immediately yields ths single particle density of states.

The procedure formulated by McMillan and Rowell is the following. One first measures the structure above the gap edge in dI/dV accurately. Next, one "guesses" an $\alpha^2F(\Omega)$, and using this guess computes $\Delta(\omega)$, and hence $dI(\omega)/dV$, using Eliashberg theory. The calculated function is compared to the experimental result, and corrections to the initial guess are computed. Corrections can be obtained through functional derivatives; the procedure amounts to a Newton-Raphson method for functions (rather than for single variables). The new $\alpha^2F(\Omega)$ is used through the procedure all over again, until the result converges. One then claims to have "measured" the underlying $\alpha^2F(\Omega)$. That this procedure works is a priori not obvious. There seems to be no reason why the solution should be unique, but apparently most of the time it is. That the result is physically meaningful is apparent because of several tests. First, that the function comes out positive is already a triumph. Negative spectral functions are not ruled out in the iterative process, so the positivity indicates a physical result (the spectral function must be positive (for positive frequency)). Although not apparent from the above description, the inversion procedure requires knowledge of the density of states in the phonon region only. Nonetheless, structure occurs well beyond the phonon region. One can then use the spectral function with Eliashberg theory to *predict* the density of states at higher energies. The agreement with the experimental result is spectacular (see Fig. 32 in Ref. [19]). Finally one can compare to neutron scattering experiments, which measure the phonon density of states, $F(\Omega)$, directly; these experiments tell us at what energies the phonons exist, but not how strongly coupled they are to the electrons. Hence, the two functions, $F(\Omega)$, and $\alpha^2F(\Omega)$, don't have to be similar in many respects, though the frequency range of the latter clearly cannot exceed that of the former. As it turns out, these functions are rather similar (and, of course, fulfill the required condition); this indicates that the coupling function $\alpha^2(\Omega) \equiv \alpha^2F(\Omega)/F(\Omega)$, is not very frequency dependent. A detailed comparison of these two probes is provided in Ref. [24].

Finally we should mention that other measurements often corroborate this story. The gap ratio often comes out in better agreement with experiment, and various thermodynamic quantities show better agreement too [23]. One might well wonder at how successful this approach has been historically, though, since important effects apparently have been omitted. For example, electron-electron Coulomb interactions have only been included insofar as they alter the underlying band structure (this is implicit), and through the single parameter μ^* (this is explicit in the theory).

Perhaps partially for the reasons mentioned in the previous paragraph, along with other aspects, such tunneling measurements have so far failed to provide conclusive results for the cuprate superconductors. In the case of the alkali-doped fullerenes, tunneling has clearly demonstrated a gap, but so far tunneling measurements have not been used to invert for $\alpha^2F(\Omega)$ [25]. Part of the prob-

lem is that the phonons are known from neutron scattering [26] to extend out to about 250 meV, much further than in conventional superconductors. For these reasons we looked for an alternate method to deduce the underlying interactions, one which uses the measured optical conductivity [27]. In the next section we briefly describe optical measurements and then describe our procedure and its application to K_3C_{60}.

Optical Properties in Metals

A common method to determine the optical conductivity is to measure the reflectance [28] as a function of frequency, usually at normal incidence. The reflectance, $R(\nu)$, is defined as the absolute ratio squared of reflected over incident electromagnetic wave amplitude. The complex reflectivity is then defined by

$$r(\nu) \equiv R(\nu) \exp\left(i\theta(\nu)\right), \tag{1}$$

where $\theta(\nu)$ is the phase, and is obtained through a Kramers-Kronig relation from the reflectance [28]

$$\theta(\nu) = \frac{\nu}{\pi} \int_0^\infty \frac{\ln R(\nu') - \ln R(\nu)}{\nu^2 - \nu'^2} d\nu'. \tag{2}$$

The complex reflectivity can be related to the complex index of refraction, $n(\nu)$,

$$r(\nu) \equiv \frac{1 - n(\nu)}{1 + n(\nu)}, \tag{3}$$

which, finally, is related to the complex conductivity, $\sigma(\nu)$ (using the dielectric function, $\epsilon(\nu)$:

$$\epsilon(\nu) \equiv n^2(\nu) = \epsilon_\infty + \frac{4\pi i \sigma(\nu)}{\nu}, \tag{4}$$

where ϵ_∞ is the dielectric function at high frequency (in principle, for infinite frequency this would be unity). It is through such transformations that the 'data' is often presented in 'raw' form. Nonetheless, assumptions are required to proceed through these steps; for example, Eq. (2) indicates quite clearly that the reflectance is required over all positive frequencies. Thus extrapolation procedures are required at low and high frequencies; a more thorough discussion can be found in [29]; see also [30].

In Figs. 1 and 2 we illustrate how elastic and inelastic scattering processes affect the reflectance. In Fig. 1 we use a simple Drude form for the complex conductivity, $\sigma(\nu) = \sigma_0/(1 - \nu\tau)$ and plot the reflectance which results from the application of the above formulae. Here the coefficient σ_0 is the dc conductivity, and the parameter $1/\tau$ is the electron elastic scattering rate. The source of elastic scattering is unspecified, but usually results from electron-impurity scattering. In Fig. 1 the plasma edge is evident, and occurs, of course, near the plasma frequency, ω_P. The "sharpness" of the dropoff decreases with

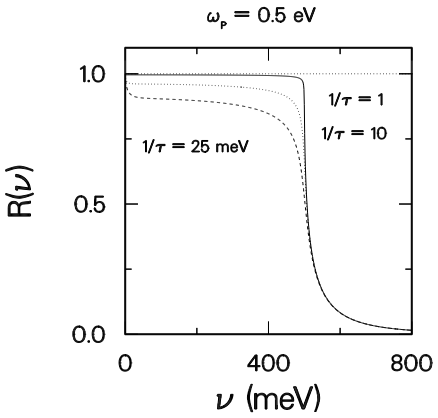

FIG. 1. The reflectance $R(\nu)$ vs. frequency for the Drude model. Three curves are shown, corresponding to the three elastic scattering rates shown.

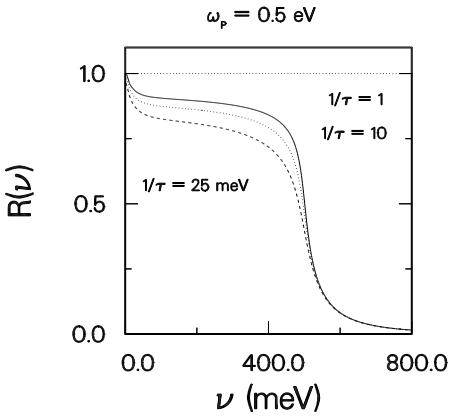

FIG. 2. The reflectance $R(\nu)$ vs. frequency for the case shown in Fig. 1, but with additional inelastic scattering (modelled through the electron-phonon interaction in Pb). Note the general rounding of the curves and the decreased reflectance (as compared with those in Fig. 1).

increasing scattering rate. The plateau region below the plasma frequency is referred to as the relaxation region; the level decreases with increasing scattering rate, as expected, since stronger scattering should cause the reflectance to decrease. Finally, at very low frequency, the Hagen-Rubens form, $R(\nu) \approx 1 - \sqrt{\frac{8}{\omega_P \tau} \frac{\nu}{\omega_P}}$ takes the reflectance smoothly to unity at zero frequency.

In Fig. 2 we use the same elastic scattering rates for the three curves shown in Fig. 1. In addition we include inelastic scattering through the electron-phonon interaction (in this case with Pb). Note that the main effect is a rounding of the edge, and a general decrease of the reflectance everywhere. The effect is very nonlocal in frequency — note that the Pb phonon spectrum extends to about 10 meV, which is tiny on the scale of this figure, and particularly on the frequency scale of the changes with respect to Fig. 1. The effect of the inelastic scattering is also cumulative, a result which follows from the fact that the effective scattering rate increases as a function of frequency [31,30].

The corresponding conductivity curves are shown in Figs 3-5. In Fig. 3 we show the Drude form (Lorentzian) for the three scattering rates shown previously. The results shown in Fig. 3 are independent of temperature. In Fig. 4 we suppress the elastic scattering rate ($1/\tau = 0$), to see more clearly the effect of inelastic scattering (here included through the electron-phonon interaction in $Ba_{1-x}K_xBiO_3$, with $T_c = 29$ K). The results shown are in the normal state only; we have referenced the temperatures to the critical temperature as a convenience only. What is clear is that at high temperatures, enough phonons are present to mimic impurity scattering, so that a "Drude-like" peak is present. At low temperatures this peak vanishes, and structure becomes more visible (solid curve in the figure). This structure provides a signature of the electron-phonon interaction, analogous to the information inherent in the structure in the tunneling I-V characteristic [32,33]. Finally, in Fig. 5, we show similar results, but with an elastic scattering rate $1/\tau = 10$ meV, so that a Drude peak remains even at zero temperature. Note that the structure remains, but is not nearly as visible as in the clean limit, and neither seems to display the degree of structure seen in tunneling. We also remark that similar statements apply to the imaginary part of the conductivity (see Ref. [34] for a full discussion).

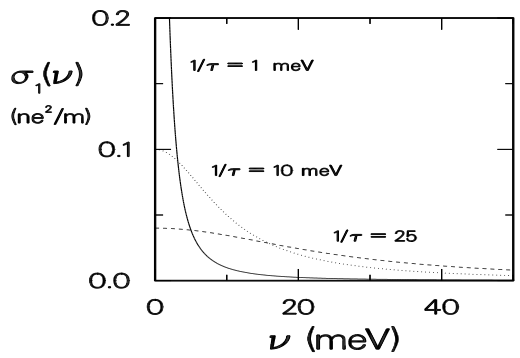

FIG. 3. The real part of the optical conductivity in the Drude model (elastic scattering only) for the same three scattering rates shown in Fig. 1. These results are independent of temperature.

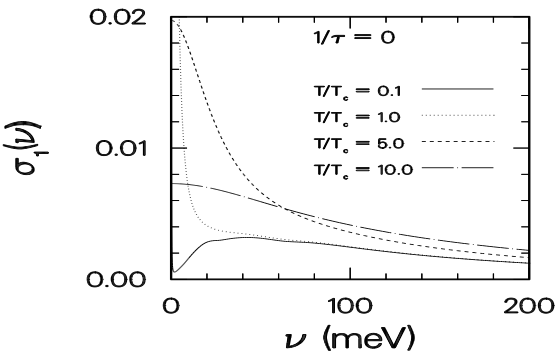

FIG. 4. The real part of the optical conductivity in the clean limit (no elastic scattering). The only source of scattering is inelastic, as modelled by the electron-phonon interaction in $Ba_{1-x}K_xBiO_3$ ($T_c = 29$ K) [32]. The curves shown are all for the normal state. Note the "Drude-like" peak at the origin at high temperatures, and its absence as the temperature approaches zero.

The Inversion of the Optical Conductivity

The inference of the electron-phonon interaction through the optical conductivity has a long history. No doubt it was apparent that the information was available right from the initial studies of Holstein [35], where he made clear that inclusion of the electron-phonon interaction would have a significant impact on the optical conductivity. The first real attempt, however, to infer

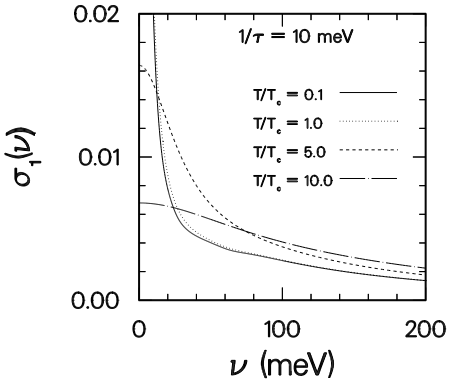

FIG. 5. The real part of the optical conductivity as in Fig. 5 but now with additional elastic scattering ($1/\tau = 10$ meV). A Drude peak is present at the origin for all temperatures. In both this figure and in Fig. 4 structure is only discernable at the lowest temperatures.

electron-phonon effects from the optical conductivity was made by Allen [36]. He was motivated by infrared measurements on superconducting Pb [37], and the possibility of inversion in that case. The result was a qualitative success, and even yielded quantitatively good results [38]. Our recent work, which we now describe, builds on the work of Ref. [36].

The remainder of this section concerns only the normal state, in contrast to tunneling, where the superconducting state was a requirement. This is both an advantage and disadvantage, as the theory we present is at zero temperature, which may be difficult to achieve in the normal state for some materials. The required expressions are [36,27]:

$$\sigma(\nu) = \frac{\omega_P^2}{4\pi}\frac{i}{\nu}\int_0^\nu d\omega \frac{1}{\nu + i/\tau - \Sigma(\omega) - \Sigma(\nu-\omega)} \tag{5}$$

where

$$\Sigma(\omega) = \int_0^\infty d\Omega \alpha^2F(\Omega)\ln|\frac{\Omega-\omega}{\Omega+\omega}| - i\pi\int_0^{|\omega|} d\Omega\ \alpha^2F(\Omega) \tag{6}$$

is the effective electron self-energy due to the electron-phonon interaction. The spectral function that appears in Eq. (6) is really a closely related function, as has been discussed by Allen [36] and Scher [39]. For our purposes we will treat them identically. Eqs. (5) and (6) elucidate why the electron-phonon signature is rather modest in the optical conductivity (it is even better hidden in the reflectance); two integrations effectively average over the electron-phonon spectral function. One would like to "unravel" this information as much as possible before attempting an inversion, so that, in effect, the signal is "enhanced". To this end one can attempt various manipulations. As a first step one can make a weak coupling type of approximation to obtain [27] the *explicit* result:

$$\alpha^2F(\nu) = \frac{1}{2\pi}\frac{\omega_P^2}{4\pi}\frac{d^2}{d\nu^2}\left\{\nu Re\frac{1}{\sigma(\nu)}\right\}. \tag{7}$$

Insofar as Eq. (7) works extremely well (as we shall see in a moment), it is a remarkable result. It tells us that, with a judicious manipulation of the conductivity data, the underlying electron-phonon spectral function emerges in closed form. This is a much better result than we were initially hoping for. Not surprisingly it requires two derivatives of the data (recall the two integrations), so in practice accurate measurements are required (actually smoothing the data works quite well — and too much smoothing cannot really give you a spurious result; at worst it will obscure an otherwise noisy result — see Ref. [40] for an early application of Eq. (7)). Perhaps the most inaccurate part is the determination of the plasma frequency, which can be obtained through a sum rule or from other measurements, procedures which are both often fraught with errors.

Before we evaluate Eq. (7) with a known example, we note that a full numerical inversion of Eqs. (5) and (6) is possible. However, a straightforward application of a Newton-Raphson iteration technique turns out to be very unstable. We derived instead the following expression [41]:

$$\alpha^2F(\nu) = \frac{1}{\pi}\mathrm{Im}\left\{\frac{2\int_0^\nu d\omega \frac{[1+\lambda(\omega)][1+\lambda(\nu-\omega)]}{[\nu+\frac{i}{\tau}-\Sigma(\omega)-\Sigma(\nu-\omega)]^3} + \frac{4\pi i}{\omega_P^2}\frac{d^2}{d\nu^2}[\nu\sigma(\nu)]}{g^2(\nu) + \frac{1}{[\nu+\frac{i}{\tau}-\Sigma(\nu)]^2}}\right\} \tag{8}$$

where

$$g(\nu) \equiv -\frac{4\pi i}{\omega_P^2}\frac{d}{d\nu}[\nu\sigma(\nu)] + \int_0^\nu d\omega \frac{1+\lambda(\omega)}{[\nu+\frac{i}{\tau}-\Sigma(\omega)-\Sigma(\nu-\omega)]^2}, \tag{9}$$

and

$$\lambda(\omega) \equiv \int_0^\infty d\Omega\alpha^2F(\Omega)\frac{2\Omega}{\Omega^2-\omega^2} \tag{10}$$

so that the right hand side depends (in many places through both $\lambda(\omega)$ and $\Sigma(\omega)$) on $\alpha^2F(\Omega)$. We have found that only a few iterations of these equations are needed, even with an initial guess which is blank. The result from this procedure in the case of Pb is plotted in Fig. 6

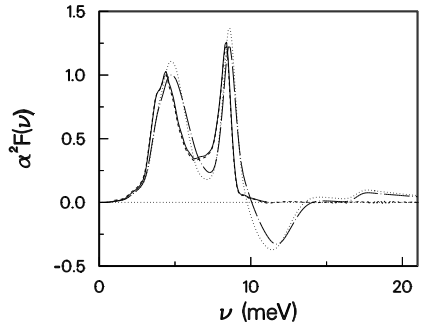

FIG. 6. $\alpha^2F(\nu)$ for Pb (solid curve) vs. ν, along with the estimates obtained from Eq. (7) with an impurity scattering rate, $1/\tau = 1$ meV (dotted) and 10 meV (dot-dashed). These are both qualitatively quite accurate, before they become negative at higher frequencies. Also plotted is the result (dashed curve, indiscernible from the solid curve) obtained from a full numerical inversion, as described in the text.

(dashed curve), though the curve is essentially indistinguishable from the tunneling density of states (solid curve) which was used to generate the optical conductivity data in the first place. This illustrates the success of the method. However, the more remarkable result is that of Eq. (7). We have also plotted the result of this formula applied to the conductivity of Pb (again generated numerically) for two values of the elastic scattering rate (after all in a real experiment we don't know what this value is). The resulting curves (dotted and dot-dashed) give very good qualitative results (and don't depend very much on the value of $1/\tau$ used). They both exhibit a spurious negative part plus some spurious "recovery" noise, so these effects teach us about the limitations of Eq. (7). If we ignore such negative pieces, we get a very good representation of the spectral function.

The Case of K_3C_{60}

For the case of K_3C_{60} we simply use the approximate Eq. (7), bearing in mind some of the limitations already discussed. We have used the reflectance data at 25 K for K_3C_{60} taken by Degiorgi *et al.* [8]. Details of our analysis of this data are given in [27]. The result of using Eq. (7) is plotted in Fig. 7 (solid curve), along with the neutron scattering data from [26] (dashed curve). We also include a result obtained through analysis of photoemission data [42] (dotted curve), where we have taken the coupling strengths and frequencies of particular phonon branches analyzed there, and arbitrarily broadened them.

Our results are in very good qualitative agreement with the neutron scattering data [26]. The energy scale is certainly correct, and moreover the peaks line up fairly well, suggesting that the coupling is not dependent on energy. Note that we have omitted some negative pieces, as these are expected to arise from the use of Eq. (7) (not the low frequency negative component, however, for which we have no satisfactory explanation at present). We also note that the agreement with the photoemission-derived results is not particularly good.

We can easily 'check' this result by computing the reflectance expected from this spectral function and comparing to the measured reflectance. The agreement is within experimental error [27]. Thus, we have demonstrated a consistent explanation of the data (but not necessarily a unique one). The fitted parameters are $\omega_P = 6000$ cm^{-1} and $1/\tau = 95$ meV for the plasma frequency and impurity scattering rate, respectively.

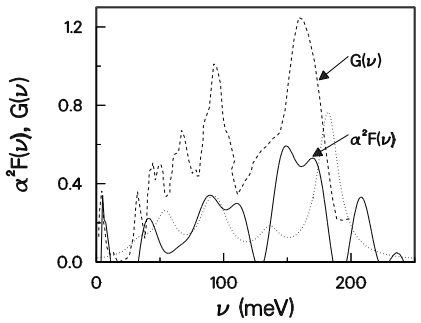

FIG. 7. The $\alpha^2F(\nu)$ for K_3C_{60} (solid curve) extracted from the reflectance data of Degiorgi *et al.* [8], using Eq. (7). For purposes of analysis we have omitted the negative parts. The neutron scattering results from Ref. [26] (dashed curve) are also shown. Clearly the energy scale in $\alpha^2F(\nu)$ matches that of the phonons, and some of the peaks even line up correctly. Finally, the dotted curve comes from an analysis of photoemission data [42], where we have arbitrarily broadened the phonon spectrum with Lorentzian lineshapes.

We have used the extracted $\alpha^2F(\nu)$ in Fig. 2 to determine whether or not such a spectral function can account

for the superconducting properties in K_3C_{60}. We find, given $T_c = 19$ K, the Coulomb repulsion pseudopotential is $\mu^* = 0.4$ (using a cut-off, $\omega_c = 1$ eV). This is in effect another check, since a negative μ^* would indicate a breakdown. The spectrum is characterized by $\lambda = 1.2$ and $\omega_{ln} = 40$ meV, parameters which give BCS-like results for superconducting properties (for example, the gap ratio comes out to be $2\Delta_0/k_BT_c \approx 4$). If the low frequency peak in $\alpha^2F(\nu)$ at 5 meV is excluded, the results are then *very* BCS-like: $\lambda = 0.8$, $\mu^* = 0.34$, $T_c/\omega_{ln} \approx 0.016$, and the gap ratio is $2\Delta_0/k_BT_c \approx 3.6$. These results are consistent with some tunneling and infrared measurements [7] but inconsistent with others [6]. The degree of coupling roughly agrees with that extracted through an analysis of photoemission data [42]. Microwave measurements may provide a more discriminating probe for the low frequency part of the spectrum, as discussed in [30].

In summary, we have described an inversion scheme to extract from the optical conductivity (or reflectance) a boson spectral function responsible for inelastic scattering in a metal. The full inversion scheme is numerical, but we have also derived an explicit expression which provides a remarkably good semi-quantitative result. We have applied this technique to K_3C_{60}, and have found the *qualitatively correct* $\alpha^2F(\nu)$ for this material. Its frequency range lies in the phonon region and peaks in $\alpha^2F(\nu)$ line up with peaks in the phonon distribution function as determined by neutron scattering. The coupling is sufficiently strong to explain the superconductivity in this material. Thus, the weak coupling approach presented here appears to be able to account for the main features observed in the far-infrared. K_3C_{60} appears to be a conventional weak coupling electron-phonon superconductor.

I would like to acknowledge my collaborators in some of this work, Tatiana Startseva and Jules Carbotte. This research was supported by the Natural Sciences and Engineering Research Council (NSERC) of Canada and by the Canadian Institute for Advanced Research (CIAR).

[1] A.F. Hebard, M.J. Rosseinsky, R.C. Haddon,D.W. Murphy, S.H. Glarum, T.T.M. Palstra, A.P. Ramirez, and A.R. Kortan, Nature **350**, 600 (1991).

[2] S. Satpathy, Chem. Phys. Lett. **130**, 545 (1986).

[3] M.S. Dresselhaus, G. Dresselhaus and P.C. Eklund, *Science of Fullerenes and Carbon Nanotubes*, (Academic Press, Toronto, 1996).

[4] See the reviews and references cited therein:
A.P Ramirez, Superconductivity Review **1**, 1 (1994).
M.P. Gelfand, Superconductivity Review **1**, 103 (1994).
W.E. Pickett, Solid State Physics **48**, 226 (1994).
C.H. Pennington and V.A. Stenger, Rev. Mod. Phys. **68**, 855 (1996).
O. Gunnarsson, Rev. Mod. Phys. **69**, 575 (1997).
L. Degiorgi, Advances in Physics, **47**, 207 (1998).

[5] X.D. Xiang, J.G. Hou, G. Briceno, W.A. Vareka, R. Mostovoy, A. Zettl, V.H. Crespi and M.L. Cohen, Science **256**, 1190 (1992).
X.D. Xiang, J.G. Hou, V.H. Crespi, A. Zettl and M.L. Cohen, Nature **361**, 54 (1993).

[6] Z. Zhang, C. Chen and C.M. Lieber, Science **254**, 1619 (1991).

[7] D. Koller, M.C. Martin, L. Mihály, G. Mihály, G. Oszányi, G. Baumgartner and L. Forró, Phys. Rev. Lett. **77**, 4082 (1996).

[8] L. Degiorgi, E.J. Nicol, O. Klein, G. Grüner, P. Wachter, S.-M. Huang, J. Wiley and R.B. Kaner, Phys. Rev. B**49**, 7012 (1994); L. Degiorgi et al. Nature **369**, 541 (1994).

[9] R.F. Keifl *et al.*, Phys. Rev. Lett. **70**, 3987 (1993).

[10] Y.J. Uemura *et al.*, Nature **352**, 605 (1991).

[11] J.P. Franck, in *Physical Properties of High Temperature Superconductors IV*, edited by D.M. Ginsberg (World Scientific, Singapore, 1994) p. 189.

[12] D. Rainer, private communication, although he notes the tunneling measurement on V with Al as a normal state metal in proximity, from which the electron-phonon interaction in Al can be inferred: J. Zasadzinski *et al.* Phys. Rev. B **25**, 1622 (1982).

[13] I. Giaever, Phys. Rev. Lett. **5**, 147 (1960).

[14] J.C. Swihart, IBM J. Research Develop. **6**, 14 (1962).

[15] G.M. Eliashberg, Zh. Eksperim. i Teor. Fiz. **38**, 966 (1960); Soviet Phys. JETP **11**, 696 (1960).

[16] J.M. Rowell, P.W. Anderson and D.E. Thomas, Phys. Rev. Lett. **10**, 334 (1963).

[17] J.R. Schrieffer, D.J. Scalapino and J.W. Wilkins, Phys. Rev. Lett. **10**, 336 (1963).

[18] W.L. McMillan and J.M. Rowell, Phys. Rev. Lett. **14**, 108 (1965).

[19] W.L. McMillan and J.M. Rowell in *Superconductivity*, edited by R.D. Parks (Marcel Dekker, New York (1969)) Vol. 1, p.561.

[20] D.J. Scalapino, in *Superconductivity*, edited by R.D. Parks (Marcel Dekker, Inc., New York, 1969)p. 449.

[21] P.B. Allen and B. Mitrović, in *Solid State Physics,* edited by H. Ehrenreich, F. Seitz, and D. Turnbull (Academic, New York, 1982) Vol. 37, p.1.

[22] D. Rainer, in *Progress in Low Temperature Physics*, Vol. 10, edited by D.F. Brewer (North-Holland, 1986), p.371.

[23] J.P. Carbotte, Rev. Mod. Phys. **62**, 1027 (1990).

[24] J.M. Rowell and R.C. Dynes, in *Phonons, Proceedings of the international conference, Rennes, France*, edited by M.A. Nusimovici (Flammarion Sciences, Paris, 1971)p. 150.

[25] J. Ostrick, with R.C. Dynes, has performed some preliminary tunneling measurements on these systems (private communication).

[26] L. Pintschovius, Rep. Prog. Phys. **57**, 473 (1996).

[27] F. Marsiglio, T. Startseva and J.P. Carbotte, Phys. Lett. A**245**, 172 (1998).

[28] T. Timusk and D.B. Tanner in *Physical Properties of High Temperature Superconductors I*, edited by D.M. Ginsberg (World Scientific, Singapore, 1989) p. 339. D.B.

Tanner and T. Timusk in *Physical Properties of High Temperature Superconductors III*, edited by D.M. Ginsberg (World Scientific, Singapore, 1992) p. 363.
[29] F. Wooten, *Optical Properties of Solids* (Academic Press, New York, 1972).
[30] F. Marsiglio and J.P. Carbotte, Aust. J. Phys. **50**, 975 (1997); Aust, J. Phys. **50**, 1011 (1997).
[31] O.V. Dolgov, E.G. Maksimov and S.V. Shulga, in *Electron-Phonon Interaction in Oxide Superconductors*, edited by R. Baquero (World Scientific, Singapore (1991)),p. 30; S.V. Shulga, O.V. Dolgov and E.G. Maksimov, Physica C **178**, 266 (1991).
[32] F. Marsiglio and J.P. Carbotte, Phys. Rev. B **52**, 16192 (1995).
[33] O.V.Dolgov, S.V.Shulga, J. of Superconductivity, **8**, 611-612 (1995).
[34] F. Marsiglio, J.P. Carbotte, A. Puchkov and T. Timusk, Phys. Rev. B**53**, 9433 (1996).
[35] T. Holstein, Phys. Rev. **96**, 535 (1954); Ann. Phys. (N.Y.) **29**, 410 (1964).
[36] P.B. Allen, Phys. Rev. B**3**, 305 (1971).
[37] R.R. Joyce and P.L. Richards, Phys. Rev. Letts. **24**, 1007 (1970).
[38] B. Farnworth and T. Timusk, Phys. Rev. B**10**, 2799 (1974); ibid B**14**, 5119 (1976).
[39] H. Scher, Phys. Rev. Lett. **25**, 759 (1970).
[40] A.V. Puchkov, D.N. Basov and T. Timusk, J. Phys. Condens. Matter **8**, 10049 (1996).
[41] F. Marsiglio, to be published in J. of Superconductivity, Erice conference proceedings: Polarons: Condensation, Pairing, Magnetism, June 1998.
[42] A.S. Alexandrov and V.V. Kabanov, Phys. Rev. B**54**, 3655 (1996).